Natural frequencies and vibrating modes for a magnetic planetary gear drive

Lizhong Xu* and Xuejun Zhu
Mechanical Engineering Institute, Yanshan University, Hebei, China

Abstract. In this paper, a dynamic model for a magnetic planetary gear drive is proposed. Based on the model, the dynamic equations for the magnetic planetary gear drive are given. From the magnetic meshing forces and torques between the elements for the drive system, the tangent and radial magnetic meshing stiffness is obtained. Using these equations, the natural frequencies and the modes of the magnetic planetary gear drive are investigated. The sensitivity of the natural frequencies to the system parameters is discussed. Results show that the pole pair number and the air gap have obvious effects on the natural frequencies. For the planetary gear number larger than two, the vibrations of the drive system include the torsion mode of the center elements, the translation mode of the center elements, and the planet modes. For the planetary gear number equal to two, the planet mode does not occur, the crown mode and the sun gear mode occur.

Keywords: Planetary drive, magnetic gear, natural frequency, mode, sensitivity

1. Introduction

The magnetic gear drive is without wear and noise, and suitable for the technical fields such as medical apparatus, chemical equipment and food processing equipment, etc. [1]. The mechanism by which magnetic force is generated in the meshing area was elucidated and an experimental meshing model was used to clarify the principle of operation of the magnetic gear [2]. The influence of the distance between the magnetic gears on the output torque for the drive was investigated [3]. The magnetic field and driving torque of the drive were also analyzed [4–6]. A parallel magnetized spur gear was described by an analytical model and the analytical model was verified with the finite element method [7]. The magnetic force gear's characteristics and the typical permanent thulium magnetism gear drive system's structure were summarized and the dynamic model of the drive system was established [8]. A new magnetic skew gear drive and a new magnetic worm gear drive using permanent magnet were proposed [9,10], and a new cycloid permanent magnetic gear drive was also proposed [11,12]. Moreover, the design and analysis of the non-contact magnet gear for conveyors were completed [13], and the application of the magnetic gear on the brushless machine for a wind power generation was also discussed [14].

As the driving torque of the magnetic gear drive is relatively small. It limits the application of the drive. Hence, a magnetic planetary gear drive was proposed, in which the speed ratio and driving torque of the drive system can be increased largely [15].

The drive consists of four basic elements as shown in Fig. 1: (a) planetary gears; (b) a sun gear; (c) a crown gear; and (d) a rotor, which forms the central output shaft upon which the planetary gears are mounted. The planetary gears and the others have permanent magnets instead of teeth. The N and S polar permanent magnets are mounted alternately on each gear. The undesirable dynamic behavior will result in unacceptable performance characteristics.

---

*Corresponding author: Lizhong Xu, Mechanical Engineering Institute, Yanshan University, Hebei, China. E-mail: xlz@ysu.edu.cn.
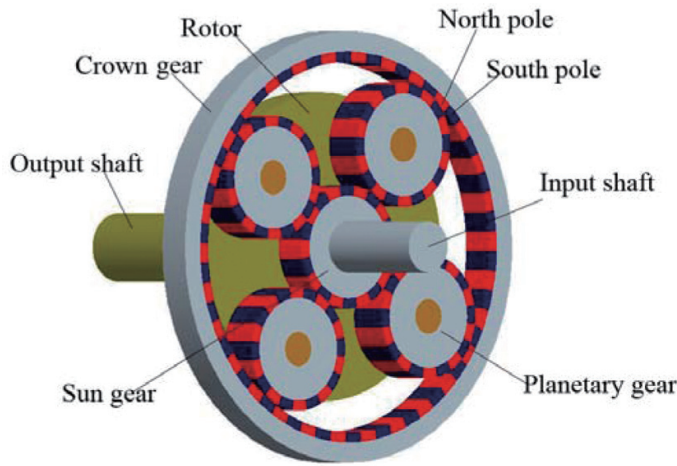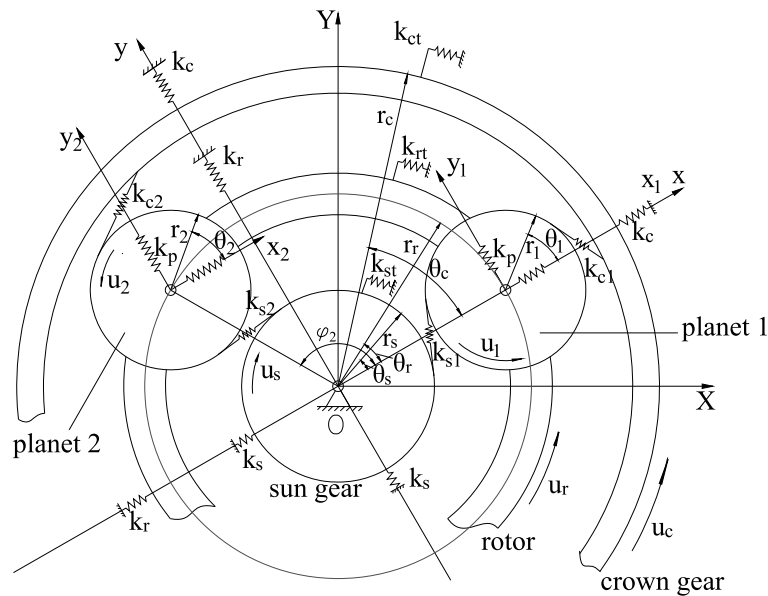
Fig. 1. The magnetic planetary drive.

Fig. 2. The dynamic model for the magnetic planetary gear drive.

The prediction of the natural frequencies and vibration modes is required in the design stage. However, the natural frequencies and vibration modes of the magnetic planetary gear drive is yet to be developed.

In this paper, the natural frequencies and vibration modes of the magnetic planetary gear drive is investigated. The authors study the problem in two steps: (1) deduce the dynamic equations for the magnetic planetary gear drive; (2) study the natural frequencies and the modes of the drive system, and the sensitivity of the natural frequencies to the system parameters.

2. Dynamic equations

The dynamic model of the magnetic planetary gear drive is shown in Fig. 2. The dynamic model employs following assumptions:

(1) Main components of the magnetic planetary gear drive are considered to be rigid, assuming that elastic deformations of these component bodies are negligible.

(2) The magnetic force between the planet gears and the sun gear or crown gear are modeled as linear meshing springs acting on the plane of action (the plane which is tangent to the rolling cylinders of the meshing elements) normal to the tooth surface. The planet supports are modeled as linear springs acting in the radial and axial directions.

(3) It is assumed that tooth separations do not occur. The tooth spacing errors and misalignments of the elements are not included in this study. Besides it, the system nonlinearities and the damping are neglected for simplifying the analysis. The rotor speed is constant.

(4) All N planet gears are assumed to be identical with the same values of mass, inertia and tooth mesh stiffness.

In Fig. 2, the coordinate system OXY is attached to the foundation, oxy to the rotor r, $o_n x_n y_n$ to the n-th planet gear. The dynamic model shown in Fig. 2 allows the crown gear, the sun gear, the rotor and each planet gear to rotate about their own rotating axes, and allows each component to translate in x_i and y_i directions. For the sake of convenience, the rotations are replaced by their corresponding translational mesh displacements as $u_i = r_i \theta_i$, $(i = s, r, c, 1, 2, \cdots N)$. Here, s denotes the sun gear, r the rotor, c the crown gear, i the planet gear, N the number of the planet gear; θ_i is the rotation angle of the sun gear, the crown gear, the planet gear or the rotor, r_i is the rolling circle radius for the sun gear, the crown gear and the planet gear, and the radius of the circle passing through planet centers for the rotor. A displacement vector $\mathbf{q}_i$ and a mass matrix $\mathbf{M}_i$ corresponding to $\mathbf{q}_i$ are then defined for each element i as

$$\mathbf{q}_i = \begin{bmatrix} x_i & y_i & u_i \end{bmatrix}^T \tag{1}$$

$$\mathbf{M}_i = diag(\begin{bmatrix} m_i & m_i & I_i/r_i^2 \end{bmatrix}) \tag{2}$$

where I_i and m_i are the polar mass moment of the inertia and mass for the element i, respectively.

2.1. Acceleration and relative displacements of the elements

Let x and y denote the components of the vector r on the coordinate system oxy, X and Y denote the components of the vector r on the fixed coordinate system OXY. Thus [16]

$$\left. \begin{array}{l} x = XC + YS \\ y = -XS + YC \end{array} \right\} \tag{3}$$

where $C = \cos \omega_r t$ and $S = \sin \omega_r t$, ω_r is the angular speed of the rotor.

From Eq. (3), the two components of the acceleration for each element can be given as

$$\left. \begin{array}{l} a_{ix} = \ddot{x}_i - 2\omega_r \dot{y}_i - \omega_r^2 x_i \\ a_{iy} = \ddot{y}_i + 2\omega_r \dot{x}_i - \omega_r^2 y_i \end{array} \right\} \quad (i = s, r, c, 1, 2, \ldots, N) \tag{4}$$

Figure 3 shows the relative displacements of the elements for the drive system(here, the rotor is not shown). From Fig. 3, the component in the meshing line of the relative displacement between the sun gear and planetary gear is [17]

$$\delta_{sn} = (x_n - x_s) \sin \varphi_{sn} + (y_s - y_n) \cos \varphi_{sn} + u_s + u_n \tag{5}$$

where x_s and y_s are the linear displacements of the sun gear in the x and y directions, respectively; $\varphi_{sn} = \varphi_n - \alpha_s$, α_s is the mesh angle between the sun gear and the planetary gear, φ_n is the angle between line oo_n and coordinate axis x direction ($\varphi_n = 2\pi(n-1)/N$, n=1,2,...,N), oo_n is the line from the center of the n-th planetary gear and the rotor center; x_n and y_n are the linear displacements of the planetary gear in the x and y directions, respectively; u_s and u_n are the tangent linear displacements of the sun gear and the planetary gear, respectively.

The component in the meshing line of the relative displacement between the planetary gear and the crown gear is

$$\delta_{cn} = (x_n - x_c) \sin \varphi_{cn} + (y_c - y_n) \cos \varphi_{cn} + u_c - u_n \tag{6}$$

where x_c and y_c are the linear displacements of the crown gear in the x and y directions, respectively; $\varphi_{cn} = \varphi_n + \alpha_c$, α_c is the mesh angle between crown gear and planetary gear; u_c is the tangent linear displacement of the crown gear.
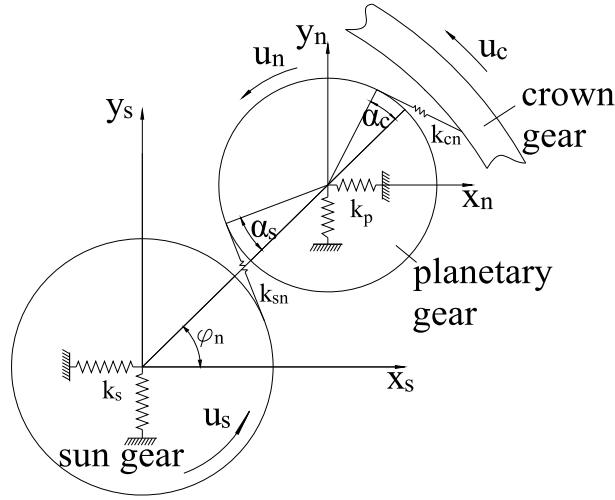
Fig. 3. Relative displacements of the elements.

The component in the x and y directions of the relative displacement between the rotor and planetary gear are

$$\delta_{rnx} = x_r - x_n - u_r \sin \varphi_n \tag{7a}$$

$$\delta_{rny} = y_r - y_n + u_r \cos \varphi_n \tag{7b}$$

The component in the tangent direction of the relative displacement between the rotor and planetary gear is

$$\delta_{rnu} = (x_n - x_r) \sin \varphi_n + (y_r - y_n) \cos \varphi_n + u_r \tag{7c}$$

2.2. Dynamic equation of the drive elements

Thus, the dynamic equations of each element can be written as [16]

$$\begin{cases} m_j(\ddot{x}_j - 2\omega_r \dot{y}_j - \omega_r^2 x_j) + \sum_{n=1}^{N} k_{jn} \delta_{jn} \sin \varphi_{jn} + k_{jr} x_j = 0 \\ m_j(\ddot{x}_j - 2\omega_r \dot{y}_j - \omega_r^2 x_j) + \sum_{n=1}^{N} k_{jn} \delta_{jn} \cos \varphi_{jn} + k_{jr} y_j = 0 \\ (I_j/r_j^2)\ddot{u}_j + \sum_{n=1}^{N} k_{jn} \delta_{jn} + k_{jt} u_j = F_j \end{cases} \tag{8}$$

where $j = r$, s and c for the rotor, the sun gear and the crown gear, respectively. The tangent load $F_j = -T_r/r_r$, T_s/r_s and 0 for the rotor, the sun gear and the crown gear, respectively. k_{jr} is the supporting stiffness in radial direction for each element. k_{jt} is the supporting stiffness in the tangent direction for each element. k_{jn} is the supporting stiffness of the bearing for the planetary gear, the meshing stiffness between the crown gear and the planetary gear, the meshing stiffness between the sun gear and the planetary gear, respectively.

Substituting Eqs (5), (6) or (7) into Eq. (8), the dynamic equations of each element can be changed into following form

$$\mathbf{M}_j \ddot{\mathbf{q}}_j + \omega_r \mathbf{G}_j \dot{\mathbf{q}}_j + \left(\mathbf{K}_{\mathbf{b}j} + \sum_n \mathbf{K}_{j\mathbf{1}}^{\mathbf{n}} - \omega_r^2 \mathbf{K}_{\Omega j} \right) \mathbf{q}_j + \sum_n \mathbf{K}_{j\mathbf{2}}^{\mathbf{n}} \mathbf{q}_j \mathbf{n} = \mathbf{F}_j \tag{9}$$

where

$$\mathbf{G}_j = -2m_j \begin{bmatrix} 0 & 1 & 0 \\ -1 & 0 & 0 \\ 0 & 0 & 0 \end{bmatrix}, \mathbf{K}_{\Omega j} = m_j \begin{bmatrix} 1 & 0 & 0 \\ 0 & 1 & 0 \\ 0 & 0 & 0 \end{bmatrix}, \mathbf{K}_{j1}^{\mathbf{n}} = k_{jn} \begin{bmatrix} 1 & 0 & -S_n \\ & 1 & C_n \\ (sym.) & & 1 \end{bmatrix},$$

$$\mathbf{K}_{j2}^{\mathbf{n}} = k_{jn} \begin{bmatrix} -1 & 0 & 0 \\ 0 & -1 & 0 \\ S_n & -C_n & 0 \end{bmatrix}, \mathbf{F}_j = \begin{bmatrix} 0 & 0 & F_j \end{bmatrix}, \mathbf{K}_{\mathbf{b}j} = diag(\begin{bmatrix} k_{jr} & k_{jr} & k_{jt} \end{bmatrix}).$$

The dynamic equations of the n-*th* planetary gear are

$$
\begin{cases}
m_p(\ddot{x}_n - 2\omega_r \dot{y}_n - \omega_r^2 x_n) + k_{sn}\delta_{sn}\sin\varphi_{sn} + k_{cn}\delta_{cn}\sin\varphi_{cn} - k_p\delta_{rnx} = 0 \\
m_p(\ddot{y}_n + 2\omega_r \dot{x}_n - \omega_r^2 y_n) - k_{sn}\delta_{sn}\cos\varphi_{sn} - k_{cn}\delta_{cn}\cos\varphi_{cn} - k_p\delta_{rny} = 0 \\
(I_p/r_p^2)\ddot{u}_n + k_{sn}\delta_{sn} - k_{cn}\delta_{cn} = 0
\end{cases}
\tag{10}
$$

Substituting Eqs (5), (6) and (7) into Eq. (10), the dynamic equations of the n-*th* planetary gear can be changed into following form

$$\mathbf{M_p\ddot{q}n} + \omega_r \mathbf{Gpn\dot{q}n} + (\mathbf{K}_{r3}^{\mathbf{n}} + \mathbf{K}_{pp}^{\mathbf{n}} - \omega_r^2 \mathbf{K}_{\Omega p})\mathbf{qn} + \mathbf{K}_{r2}^{\mathbf{n}'}\mathbf{qc} + \mathbf{K}_{c2}^{\mathbf{n}'}\mathbf{qr} + \mathbf{K}_{S2}^{\mathbf{n}'}\mathbf{qs} = 0 \tag{11}$$

where

$$\mathbf{K}_{pp}^{\mathbf{n}} = \mathbf{K}_{r3}^{\mathbf{n}} + \mathbf{K}_{s3}^{\mathbf{n}}(n = 1, 2, \ldots, N), \mathbf{K}_{s3}^{\mathbf{n}} = k_{sn} \begin{bmatrix} S_{sn}^2 & -S_{sn}C_{sn} & S_{sn} \\ & C_{sn}^2 & -C_{sn} \\ (sym.) & & 1 \end{bmatrix},$$

$$\mathbf{K}_{c3}^{\mathbf{n}} = k_{cn} \begin{bmatrix} S_{cn}^2 & -S_{cn}C_{cn} & -S_{cn} \\ & C_{cn}^2 & C_{cn} \\ (sym.) & & 1 \end{bmatrix}, \mathbf{K}_{r3}^{\mathbf{n}} = \begin{bmatrix} 1 & 0 & 0 \\ & 1 & 0 \\ (sym.) & & 0 \end{bmatrix},$$

$$C_n = \cos\varphi_n, S_n = \sin\varphi_n, C_{sn} = \cos\varphi_{sn}, S_{sn} = \sin\varphi_{sn}, C_{cn} = \cos\varphi_{cn}, S_{cn} = \sin\varphi_{cn}.$$

Combining Eqs (9) and (11), the dynamic equations of the drive system can be obtained

$$\mathbf{M\ddot{q}} + \omega_r \mathbf{G\dot{q}} + (\mathbf{K_b} + \mathbf{K_m} - \omega_r^2 \mathbf{K_\Omega})\mathbf{q} = \mathbf{T} \tag{12}$$

where $\mathbf{q}$ is the generalized coordinate vector of the drive system

$$\mathbf{q} = [x_r \quad y_r \quad u_r \quad x_c \quad y_c \quad u_c \quad x_s \quad y_s \quad u_s \quad x_1 \quad y_1 \quad u_1 \quad x_2 \quad y_2 \quad u_2 \quad \ldots \quad x_N \quad y_N \quad u_N]^T$$

$\mathbf{M}$ is the mass matrix of the drive system,

$$\mathbf{M} = diag \begin{bmatrix} \mathbf{M}_r & \mathbf{M}_c & \mathbf{M_s} & \mathbf{M_1} & \mathbf{M_2} & \ldots & \mathbf{M_N} \end{bmatrix}^T$$

$$\mathbf{M_j} = diag \begin{bmatrix} m_j & m_j & I_j/r_j^2 \end{bmatrix} \quad (j = r, c, s, 1, 2, \ldots, N)$$

$\mathbf{G}$ is the gyro matrix, it is an anti-symmetric matrix, most of its elements is zero, the nonzero elements are $G_{12} = -2m_r, G_{45} = -2m_c, G_{78} = -2m_s$ and $G_{7+3n,8+3n} = -2m_p \quad (n = 1, 2, \ldots, N)$

$\mathbf{K}_\Omega$ is the centripetal stiffness matrix

$$\mathbf{K}_\Omega = diag [m_r \quad m_r \quad 0 \quad m_c \quad m_c \quad 0 \quad m_s \quad m_s \quad 0 \quad m_p \quad m_p \quad 0 \quad \ldots \quad m_p \quad m_p \quad 0]$$

$\mathbf{K_b}$ is the supporting stiffness matrix

$$\mathbf{K_b} = \begin{bmatrix} K_{br} + \sum_n K_{r1}^n & 0 & 0 & K_{r2}^1 & K_{r2}^2 & \cdots & K_{r2}^N \\ & K_{bc} & 0 & 0 & 0 & \cdots & 0 \\ & & K_{bs} & 0 & 0 & \cdots & 0 \\ & & & K_{r3}^1 & 0 & \cdots & 0 \\ & & & & K_{r3}^2 & \cdots & 0 \\ & & & & & \ddots & \\ (sym.) & & & & & & K_{r3}^N \end{bmatrix}$$

$\mathbf{K_m}$ is the meshing stiffness matrix

$$\mathbf{K_m} = \begin{bmatrix} 0 & 0 & 0 & 0 & 0 & \cdots & 0 \\ & \sum_n \mathrm{K}_{c1}^n & 0 & \mathrm{K}_{c2}^1 & \mathrm{K}_{c2}^2 & \cdots & \mathrm{K}_{c2}^N \\ & & \sum_n \mathrm{K}_{s1}^n & \mathrm{K}_{s2}^1 & \mathrm{K}_{s2}^2 & \cdots & \mathrm{K}_{s2}^N \\ & & & \mathrm{K}_{pp}^1 & 0 & \cdots & 0 \\ & & & & \mathrm{K}_{pp}^2 & \cdots & 0 \\ & & & & & \ddots & \\ & \text{(sym.)} & & & & & \mathrm{K}_{pp}^N \end{bmatrix}$$

$\mathbf{T}$ is the load excitation vector,

$$\mathbf{T} = \begin{bmatrix} 0 & 0 & -T_r/r_r & 0 & 0 & 0 & 0 & 0 & T_s/r_s & 0 & 0 & 0 & \ldots & 0 & 0 & 0 \end{bmatrix}^T$$

The dynamic model shown in Fig. 2 allows the crown gear, the sun gear, the rotor and each planet gear to rotate about their own rotating axes, and allows each component to translate in x_i and y_i directions. It means that three DOF occur for each element. Thus, 9 DOF occur for the crown gear, the sun gear, and the rotor. 3N DOF occur for N planet gears. Therefore, Eq. (12) includes 3N+9 equations.

If the angular speed ω_r of the rotor is not large, the terms $\omega_r G \dot{q}$ and $-\omega_r^2 K_\Omega q$ can be neglected. Thus, Eq. (12) can be changed into

$$\mathbf{M\ddot{q} + Kq = T} \tag{13}$$

where

$$\mathbf{K} = \begin{bmatrix} K_{br} + \sum_n \mathrm{K}_{r1}^n & 0 & 0 & K_{r2}^1 & K_{r2}^2 & \cdots & K_{r2}^N \\ & K_{bc} + \sum_n \mathrm{K}_{c1}^n & 0 & \mathrm{K}_{c2}^1 & \mathrm{K}_{c2}^2 & \cdots & \mathrm{K}_{c2}^N \\ & & K_{bs} + \sum_n \mathrm{K}_{s1}^n & \mathrm{K}_{s2}^1 & \mathrm{K}_{s2}^2 & \cdots & \mathrm{K}_{s2}^N \\ & & & \mathrm{K}_{pp}^1 + K_{r3}^1 & 0 & \cdots & 0 \\ & & & & \mathrm{K}_{pp}^2 + K_{r3}^2 & \cdots & 0 \\ & & & & & \ddots & \\ & \text{(sym.)} & & & & & \mathrm{K}_{pp}^N + K_{r3}^N \end{bmatrix}$$

3. Magnetic meshing stiffness

If the permanent tooth is simplified as the equivalent volume current and area current, the torque caused by other outer magnetic field can be calculated as [15]

$$\vec{T} = \int_V \vec{r}' \times (\vec{J}_m \times \vec{B}_{ext}) dV' + \int_s \vec{r}' \times (\vec{j}_m \times \vec{B}_{ext}) ds' \tag{14}$$

where $\vec{B}_{ext}$ is the induction intensity vector of the outer magnetic field, $\vec{j}_m$ the equivalent area current intensity, $\vec{r}$ the position vector of one point outside the gear tooth, $\vec{r}'$ the position vector of one point inside gear tooth or on its surface, dV' and ds' the volume unit and area unit, respectively.

Supposing that the crown gear tooth is fixed and the rotating angle of the planetary gear is θ_p, and then the magnetic torque $T_{pc}(\theta_p)$ between one tooth of the planetary gear and one tooth of the crown gear can be given. Based on $T_{pc}(\theta_p)$, the tangent magnetic meshing stiffness between the planetary gear and the crown gear can be obtained as below

$$k_{pct} = \frac{1}{r^2} \cdot \frac{\partial T_{pc}}{\partial \theta_p} \tag{15}$$

The magnetic torque $T_{ps}(\theta_p)$ between one tooth of the planetary gear and one tooth of the sun gear s can be given from Eq. (14) as well. Based on $T_{ps}(\theta_p)$, the tangent magnetic meshing stiffness between the planetary gear and the sun gear can be obtained

$$k_{pst} = \frac{1}{r^2} \cdot \frac{\partial T_{ps}}{\partial \theta_p} \tag{16}$$

The radial magnetic force caused by planet gear magnetic field can be calculated as

$$F_r = \int_s (j_m \times \vec{B}_{ext}) ds' \tag{17}$$

The radial magnetic meshing stiffness between the planetary gear and the sun gear or the crown can be obtained

$$k_{jnr} = \frac{\partial F_{rj}}{\partial d} \tag{18}$$

where $j = c$ for the planetary gear and the crown, $j = s$ for the planetary gear and the sun gear.

4. Sensitivity of the magnetic planetary gear drive

The associated eigenvalue problem of Eq. (13) is obtained from the separable solution $\mathbf{q} = \phi_i e^{i\omega_i t}$

$$(\mathbf{K} - \omega_i^2 \mathbf{M})\phi_i = \mathbf{0} \tag{19}$$

where ω_i are the natural frequencies.

Equation (19) is multiplied by vector ϕ_i^T on left and changed into the following form

$$\phi_i^T (\mathbf{K} - \omega_i^2 \mathbf{M})\phi_i = 0 \tag{20}$$

Differentiation of Eq. (20) with respect to a model parameter t gives

$$\frac{\partial \phi_i^T}{\partial t}(\mathbf{K} - \omega_i^2 \mathbf{M})\phi_i + \phi_i^T \left(\frac{\partial \mathbf{K}}{\partial t} - \frac{\partial(\omega_i^2 \mathbf{M})}{\partial t} \right) \phi_i + \phi_i^T (\mathbf{K} - \omega_i^2 \mathbf{M})\frac{\partial \phi_i}{\partial t} = 0 \tag{21}$$

Substituting $\phi_i^T (K - \omega_i^2 M) = 0$ into Eq. (21), yields

$$\phi_i^T \left[\frac{\partial \mathbf{K}}{\partial t} - 2\omega_i \frac{\partial \omega_i}{\partial t}\mathbf{M} - \omega_i^2 \frac{\partial \mathbf{M}}{\partial t} \right] \phi_i = 0 \tag{22}$$

From Eq. (22), ones give

$$\frac{\partial \omega_i}{\partial t} = \frac{1}{2a_i} \left(\frac{1}{\omega_i}\phi_i^T \frac{\partial \mathbf{K}}{\partial t}\phi_i - \omega_i \phi_i^T \frac{\partial \mathbf{M}}{\partial t}\phi_i \right) \tag{23}$$

where $a_i = \phi_i^T \mathbf{M}\phi_i$

5. Results and discussion

5.1. Natural frequency and modes

By equations given in this paper, the natural frequency and vibrating modes of the magnetic planetary gear drive are investigated. The parameters of the drive system are given in Table 1. Tables 2 and 3 list the natural frequencies for different numbers of planets. The Table 2 is for $N = 4$ and 5, and the Table 3 for $N = 2$. Table 4 shows the three modes of the drive system for $N = 4$. From Tables 2–4, ones know:

Table 1
Parameters of the example system

Parameters	Rotor	Crown gear	Sun gear	Planetary gear
mass/kg	0.5393	0.4556	0.078	0.078
I_i/r_i^2/kg	0.2696	0.0595	0.0385	0.0385
r_i/mm	36.1	60	18	18
k_{pr}/(N/m)	5×10^3	5×10^3	5×10^3	5×10^3
k_{pt}/(N/m)	0	5×10^4	0	0
Mesh stiffness/(N/m)		1.8707×10^4	1.0167×10^4	
Mesh angle/($^\circ$)			44	

Table 2

Natural frequencies with multiplicity m (rad/s)

N	4	5
$m = 1$	0	0
Torsion mode of	222	222
central elements	328	348
	494	479
	1186	1290
	1634	1734
$m = 2$	126	84
Translation mode of	235	126
central elements	302	235
	658	317
	871	692
	1054	1072
$m = $ N–3	226	226
Planetary gear mode	484	484
	981	981
Order number of natural frequency ($3N + 9$)	21	24

Table 3

Natural frequencies with multiplicity m (rad/s)

N	2
$m = 1$	0
Torsion mode of	219
central elements	267
	539
	957
	1399
$m = 1$	81
Translation mode of	95
central elements	135
	255
	283
	658
	1054
$m = 1$ Crown mode	105
$m = 1$ Sun gear mode	253
Order number of natural frequency($3N + 9$)	15

(1) Six natural frequencies always have multiplicity $m = 1$ for different N. Except for the zero natural frequency(it corresponds to the rigid motion of the drive system), most of their values changes as additional planets are introduced. Their associated vibration modes have the rotation of the center elements, and the translation in x and y directions does not occur, so these modes are named the torsion mode of the center elements. In a torsion mode of the center elements, all planets have the same motion and move in phase(see Fig. 4). In Fig. 4, existing vibrations and the relationship between their dynamic displacement directions are shown for each vibration mode. Sign is used to show the phase relationship between the vibration directions of the components. However the vibration magnitude is not shown. Actually, the vibration direction and magnitude in the same figure are identical for different planets under each mode.

(2) Six natural frequencies always have multiplicity $m = 2$ for different N. Their associated vibration modes have the translation of the center elements in x and y directions, and the rotation of the center elements does not occur, so these modes are named the translation mode of the center elements(see Fig. 5). For each natural frequency, two modes correspond to it.

(3) Three natural frequencies have multiplicity $m = N-3$ and exist as long as $N > 2$. These natural frequencies are independent of the numbers of planets. Their associated vibration modes are termed the planet modes because the center elements do not move. Only the planet motion occurs in these modes (see Fig. 6). For each of these three natural frequencies, the corresponding vibration modes span a $m = N-3$ dimensional eigenspace.

(4) For $N = 2$, the multiplicity of the natural frequencies does not exist and the planetary gear modes do not occur as well. Six natural frequencies correspond to the torsion modes of the center elements. The translation modes of the center elements include seven natural frequencies. Besides it, two special modes occur. One is only for the translation of the crown gear in x and y directions, and other vibrations do not exist. The mode is

Table 4
The three modes of the drive system for $N = 4$

Natural frequency	494 rad/s	871 rad/s	981 rad/s
ϕ_{cx}	0.0000	0.2170	0.0000
ϕ_{cy}	0.0000	−0.8470	0.0000
ϕ_{cu}	0.2803	0.0000	0.0000
ϕ_{rx}	0.0000	0.7473	0.0000
ϕ_{ry}	0.0000	−0.3420	0.0000
ϕ_{ru}	−1.0000	0.0000	0.0000
ϕ_{sx}	0.0000	−0.1849	0.0000
ϕ_{sy}	0.0000	−0.1806	0.0000
ϕ_{su}	0.7155	0.0000	0.0000
ϕ_{1x}	0.3556	0.2427	0.3668
ϕ_{1y}	−0.6415	−0.7712	−0.1399
ϕ_{1u}	−0.7655	−0.0726	−1.0000
ϕ_{2x}	0.6415	0.2109	−0.1399
ϕ_{2y}	0.3556	−1.0000	−0.3668
ϕ_{2u}	−0.7655	−0.8552	1.0000
ϕ_{3x}	−0.3556	0.2427	−0.3668
ϕ_{3y}	0.6415	−0.7712	0.1399
ϕ_{3u}	−0.7655	0.0726	−1.0000
ϕ_{4x}	−0.6415	0.2109	0.1399
ϕ_{4y}	−0.3556	−1.0000	0.3668
ϕ_{4u}	−0.7655	0.8552	1.0000
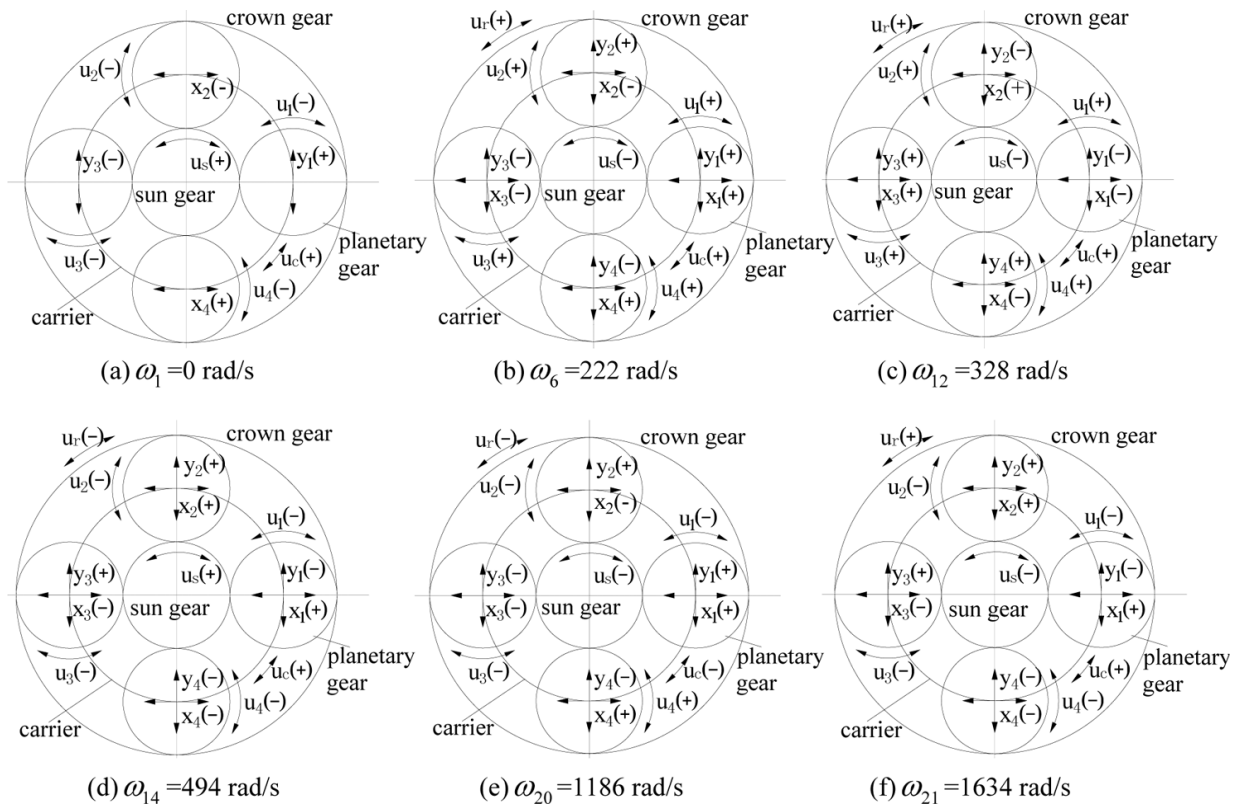
Fig. 4. Torsion modes of the central elements ($N = 4$).
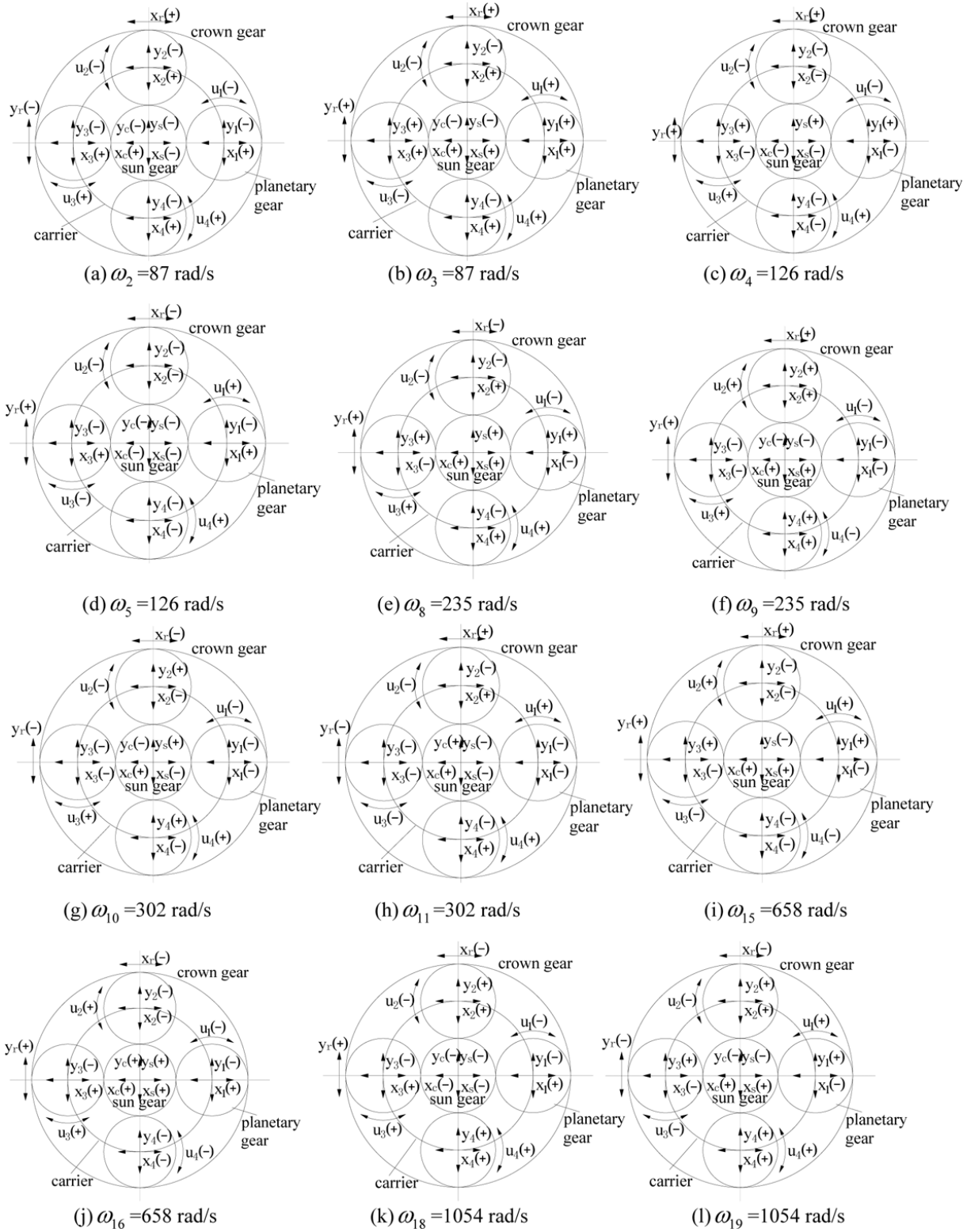
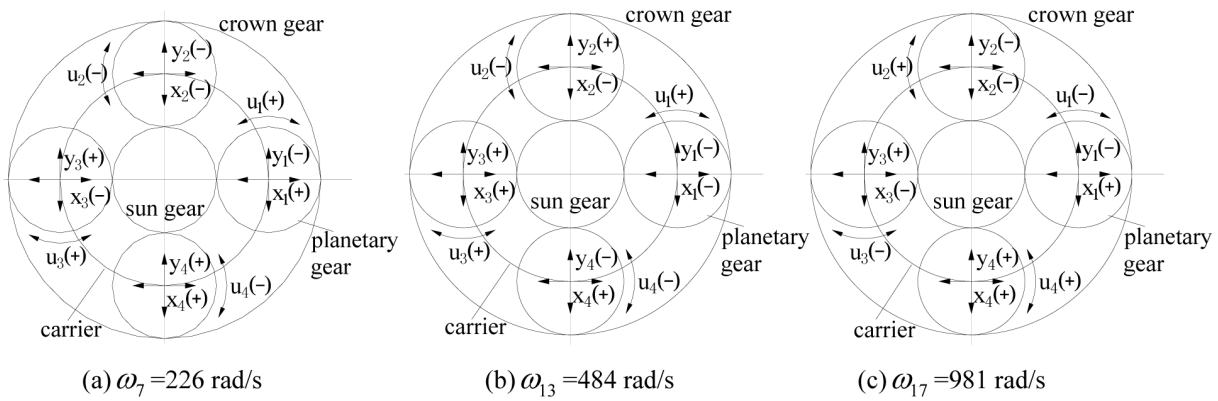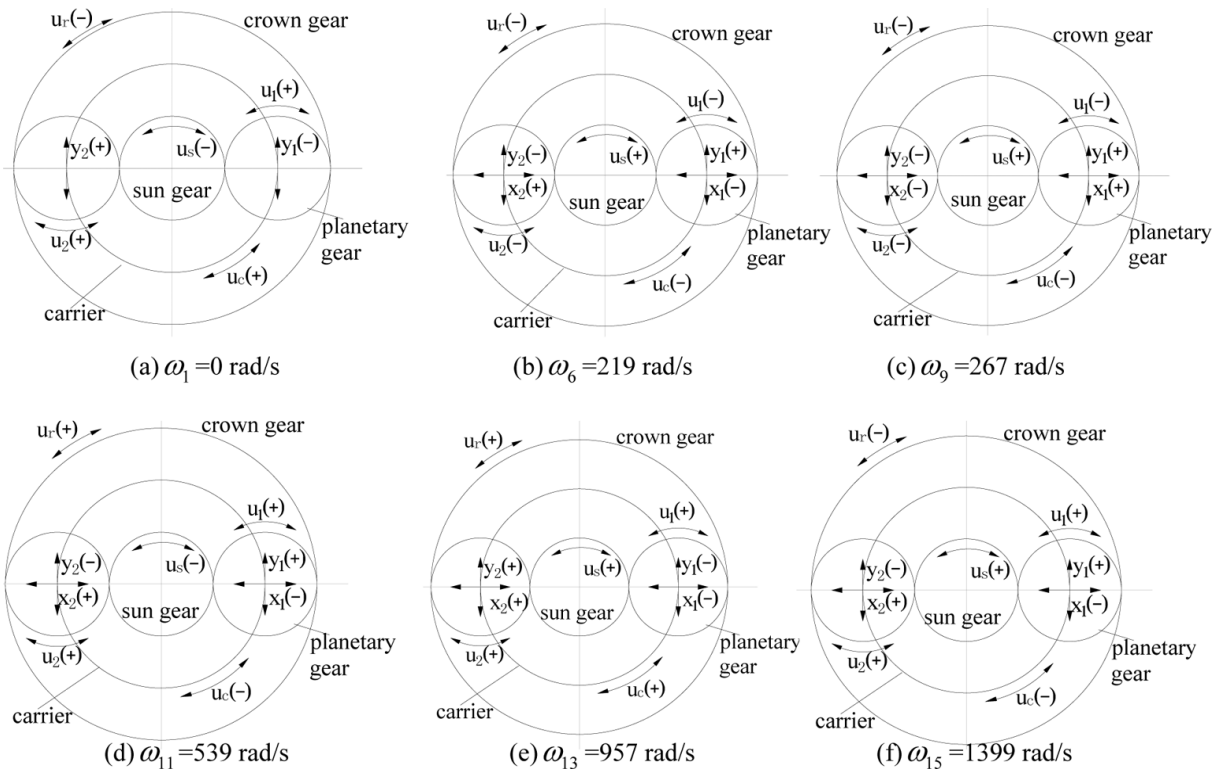Fig. 5. Translation modes of the central elements ($N = 4$).

(a) $\omega_7 = 226$ rad/s   (b) $\omega_{13} = 484$ rad/s   (c) $\omega_{17} = 981$ rad/s

Fig. 6. Planetary gear modes ($N = 4$).

(a) $\omega_1 = 0$ rad/s   (b) $\omega_6 = 219$ rad/s   (c) $\omega_9 = 267$ rad/s

(d) $\omega_{11} = 539$ rad/s   (e) $\omega_{13} = 957$ rad/s   (f) $\omega_{15} = 1399$ rad/s

Fig. 7. Torsion modes of the central elements ($N = 2$).

called as the crown mode. Another is only for the translation of the sun gear in x and y directions, and other vibrations do not exist which is called as the sun gear mode(see Table 3 and Figs 7–9).

The effects of the rotor speed on the natural frequencies of the drive system are investigated(see Table 5). It shows:

(1) As the rotor speed grows, the natural frequencies of the drive system drop for the different modes. The larger is the rotor speed, the more obviously the natural frequencies drop. For mode 1 of the translation mode of central elements, the natural frequency decreases by 0.63% when the rotor speed increases from 0 to 10 rad/s. For the same mode, the natural frequency decreases by 28.5% when the rotor speed increases from 70 to 80 rad/s.
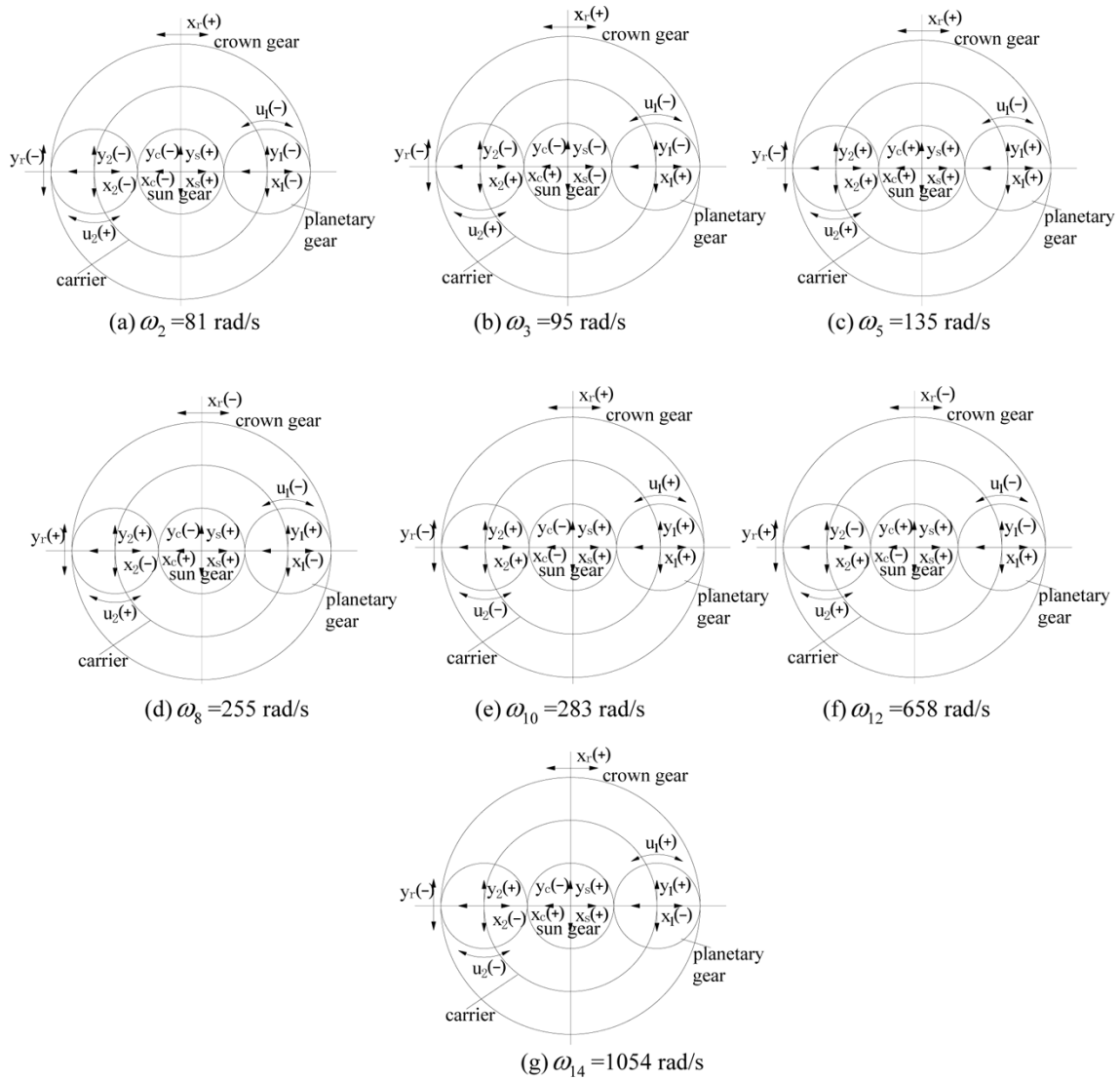
(a) $\omega_2 = 81$ rad/s   (b) $\omega_3 = 95$ rad/s   (c) $\omega_5 = 135$ rad/s

(d) $\omega_8 = 255$ rad/s   (e) $\omega_{10} = 283$ rad/s   (f) $\omega_{12} = 658$ rad/s

(g) $\omega_{14} = 1054$ rad/s
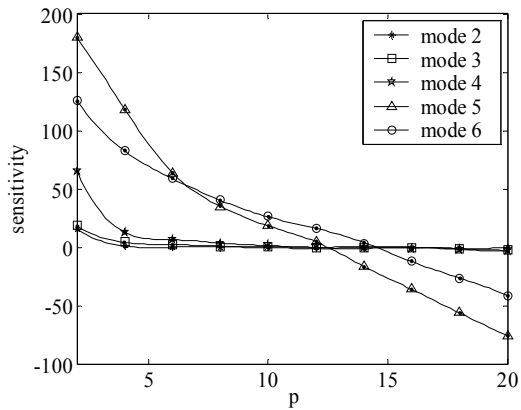
Fig. 8. Translation modes of the central elements ($N = 2$).

$\omega_4 = 105$ rad/s $\omega_7 = 253$ rad/s

(a) Crown gear mode(N=2)   (b) Sun gear mode(N=2)
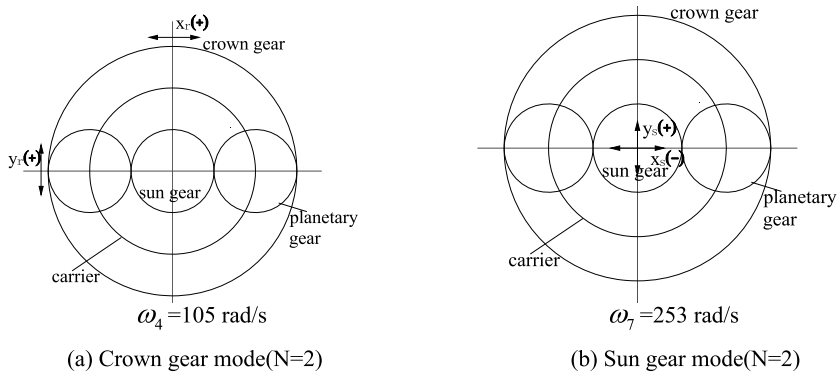
Fig. 9. (a) Crown gear mode ($N = 2$); (b) Sun gear mode ($N = 2$).

Table 5
The effects of the rotor speed on the natural frequencies(rad/s) of the drive system

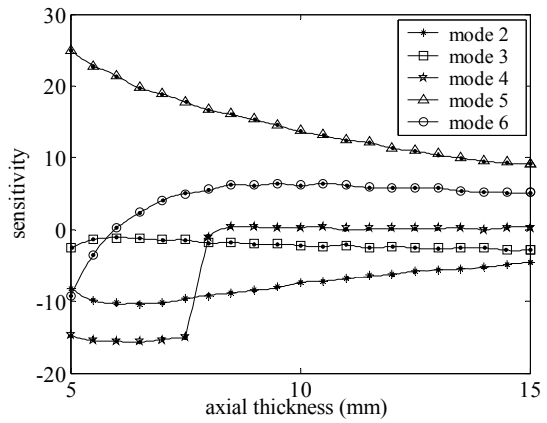| ω_r	Torsion mode of central elements					Translation mode of central elements						Planetary gear mode		
Rad/s	mode2	mode3	mode4	mode5	mode6	mode1	mode2	mode3	mode4	mode5	mode6	mode1	mode2	mode3
0	222.43	327.90	493.94	1186.1	1633.7	87.09	125.99	234.92	301.83	657.94	1053.6	225.86	483.89	981.43
10	222.28	327.87	493.89	1186.1	1633.7	86.54	125.64	234.73	301.68	657.86	1053.5	225.69	483.79	981.41
20	221.80	327.75	493.75	1186.1	1633.7	84.89	124.57	234.18	301.20	657.64	1053.5	225.17	483.48	981.38
30	221.01	327.57	493.52	1186.1	1633.7	82.05	122.78	233.24	300.40	657.26	1053.4	224.30	482.98	981.32
40	219.90	327.31	493.19	1186.1	1633.6	77.90	120.21	231.94	299.28	656.73	1053.3	223.07	482.27	981.23
50	218.45	326.98	492.76	1186.0	1633.6	72.21	116.84	230.24	297.83	656.05	1053.2	221.48	481.35	981.12
60	216.66	326.59	492.24	1186.0	1633.6	64.56	112.58	228.15	296.06	655.21	1053.0	219.53	480.23	980.99
70	214.51	326.14	491.64	1185.9	1633.6	54.12	107.33	225.67	293.94	654.23	1052.8	217.19	478.91	980.83
80	211.98	325.62	490.94	1185.9	1633.5	38.67	100.93	222.76	291.49	653.08	1052.5	214.46	477.37	980.65
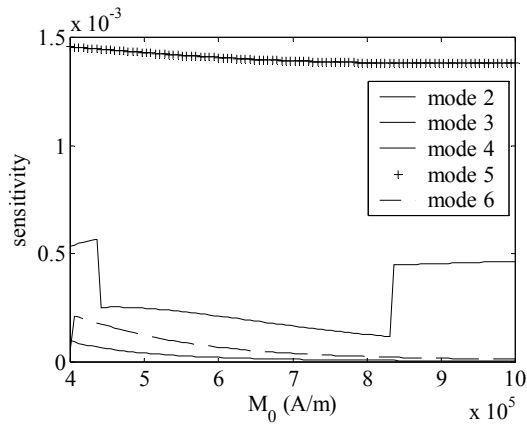
(a) M_0 changes

(b) p changes
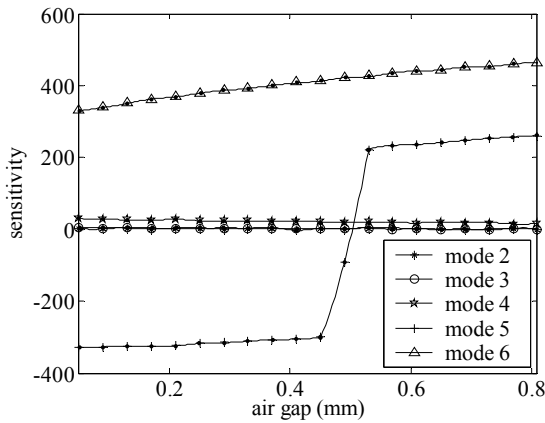
(c) air gap changes

(d) axial tooth thickness changes

Fig. 10. Sensitivity to the system parameters for the torsion modes of the central elements.

(2) For high order modes, the natural frequency decreases slightly. For mode 6 of the translation mode of central elements, the natural frequency decreases only by 0.1% when the rotor speed increases from 0 to 80 rad/s. For low order modes, the natural frequency decreases significantly. For mode 1 of the translation mode of central elements, the natural frequency decreases by 55.6% when the rotor speed increases from 0 to 80 rad/s.

5.2. Sensitivity of natural frequencies to system parameters

5.2.1. Torsion modes of the central elements

For the torsion modes of the central elements, the changes of the sensitivity along with the system parameters are given in Fig. 10. It shows:

(1) The sensitivity parameter of the natural frequencies to the magnetization intensity of the magnetic tooth is small. It shows that the magnetization intensity has little effects on the natural frequencies for the modes.

As the magnetization intensity changes, the sensitivity parameters are positive. It shows that the natural frequencies for the modes grow with increasing the magnetization intensity.

Compared to the 2–4th natural frequencies, the 5–6th natural frequencies have relatively large sensitivity to the magnetization intensity.

The sensitivity curve of the 5-th order mode intersects the sensitivity curve of the 6-th order mode at point A. It shows that the 5-th order natural frequency grows quicker than the 6-th order natural frequency with increasing the magnetization intensity in front of point A. Behind the point A, the 6-th order natural frequency grows quicker than the 5-th order natural frequency with increasing the magnetization intensity.

(2) The sensitivity parameter of the natural frequencies to the pole pair number of the worm coils is large. It shows that the pole pair number has significant effects on the natural frequencies.

The pole pair number has more obvious effects on higher order natural frequencies of the torsion modes of the central elements.

As the pole pair number grows, the 2–4th order natural frequencies for the torsion modes of the central elements first grow, and then they do not change generally. As the pole pair number grows, the 5–6th order natural frequencies for the torsion modes of the central elements first grow, and get to a maximum value, and then drop.

(3) The sensitivity parameter of the natural frequencies to the air gap is large. It shows that the air gap has significant effects on the natural frequencies for the modes as well.

The sensitivity parameters for the 2–4th modes are small, and the sensitivity parameters for the 5–6th modes are large. It means that the air gap has more obvious effects on the 5–6th order natural frequencies than those of the 2–4th modes.

As the air gap grows, the 2–4th order natural frequencies grow quite slowly. As the air gap grows, the 5th order natural frequency first drops, and then grows. As the air gap grows, the 6th order natural frequency grows obviously.

(4) Compared to the pole pair number of the worm coils and the air gap, the sensitivity of the natural frequencies to the tooth thickness of the magnetic gear is small, but it is larger than that of the magnetization intensity.

As the tooth thickness grows, the 2–3th order natural frequencies drop slowly, and the 5th order natural frequency grows. As the tooth thickness grows, the 4th and the 6th order natural frequencies first drop, and then grow.

5.2.2. Translation modes of the central elements

For the translation modes of the central elements, changes of the sensitivity along with the system parameters are given in Fig. 11. It shows:

(1) The sensitivity parameter of the natural frequencies to the magnetization intensity of the magnetic tooth is also small. It is large to the pole pair number of the worm coils or the air gap. It is moderate to the tooth thickness of the magnetic gear. This shows that the pole pair number and the air gap have more obvious effects on the natural frequencies than the magnetization intensity or the tooth thickness.

(2) As the magnetization intensity grows, the natural frequencies grow, and the 5th and the 6th natural frequencies change more obviously. On the sensitivity curve of the 5-th order mode, there is one step. It shows that the 5-th order natural frequency grows quicker with increasing the magnetization intensity behind step.

(3) The pole pair number has more obvious effects on the 5–6th order natural frequencies than those of the other order modes as well. As the pole pair number grows, the 5–6th order natural frequencies first grow, and get to a maximum value, and then drop as well.
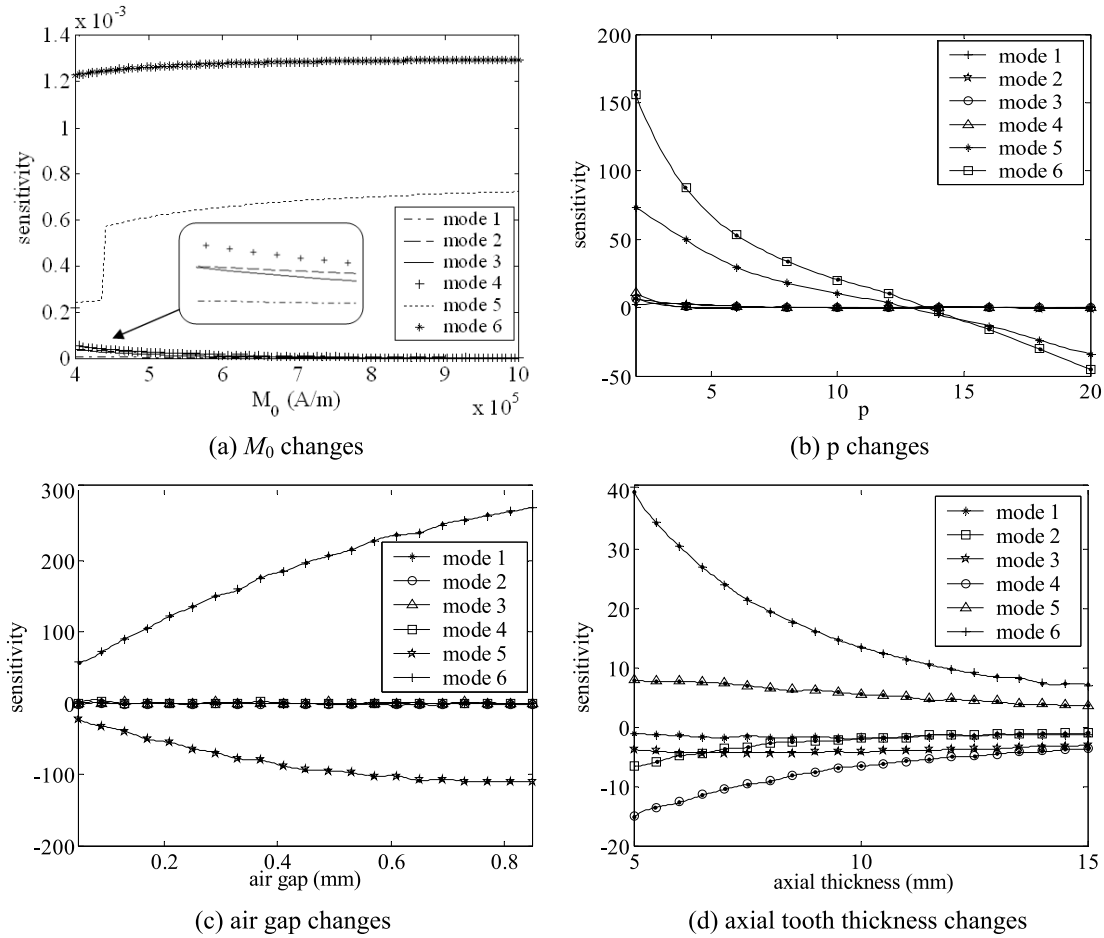
Fig. 11. Sensitivity to the system parameters for the translation modes of the central elements.

(4) As the air gap grows, the 1–4th order natural frequencies do not change nearly, the 5th order natural frequency drops, and the 6th natural frequency grows.

(5) As the tooth thickness grows, the 1–4th order natural frequencies drop, and the 5–6th order natural frequencies grow. The sensitivity parameter of the 6th natural frequencies to the tooth thickness is the largest. As the tooth thickness is small, the sensitivity parameter is relatively large. As the tooth thickness grows, the sensitivity parameter drops obviously.

5.2.3. Planet modes

For the planet modes, changes of the sensitivity along with the system parameters are given in Fig. 12. It shows:

(1) The sensitivity parameter of the natural frequencies to the magnetization intensity of the magnetic tooth is also small. It is large to the pole pair number of the worm coils or the air gap. It is moderate to the tooth thickness of the magnetic gear as well. This also shows that the pole pair number and the air gap have more obvious effects on the natural frequencies than the magnetization intensity or the tooth thickness.

(2) As the magnetization intensity grows, the 3th natural frequency grows obviously, the 1st natural frequency does not change nearly. On the sensitivity curve of the 2-th order mode, there is one step. It shows that the 2-th order natural frequency grows quicker with increasing the magnetization intensity in front of the step.

(3) As the pole pair number grows, the 1th order natural frequency first grows, and then does not change nearly. The pole pair number has more obvious effects on the 2–3th order natural frequencies. As the pole pair number grows, the 2–3rd order natural frequencies first grow, and get to a maximum value, and then drop.
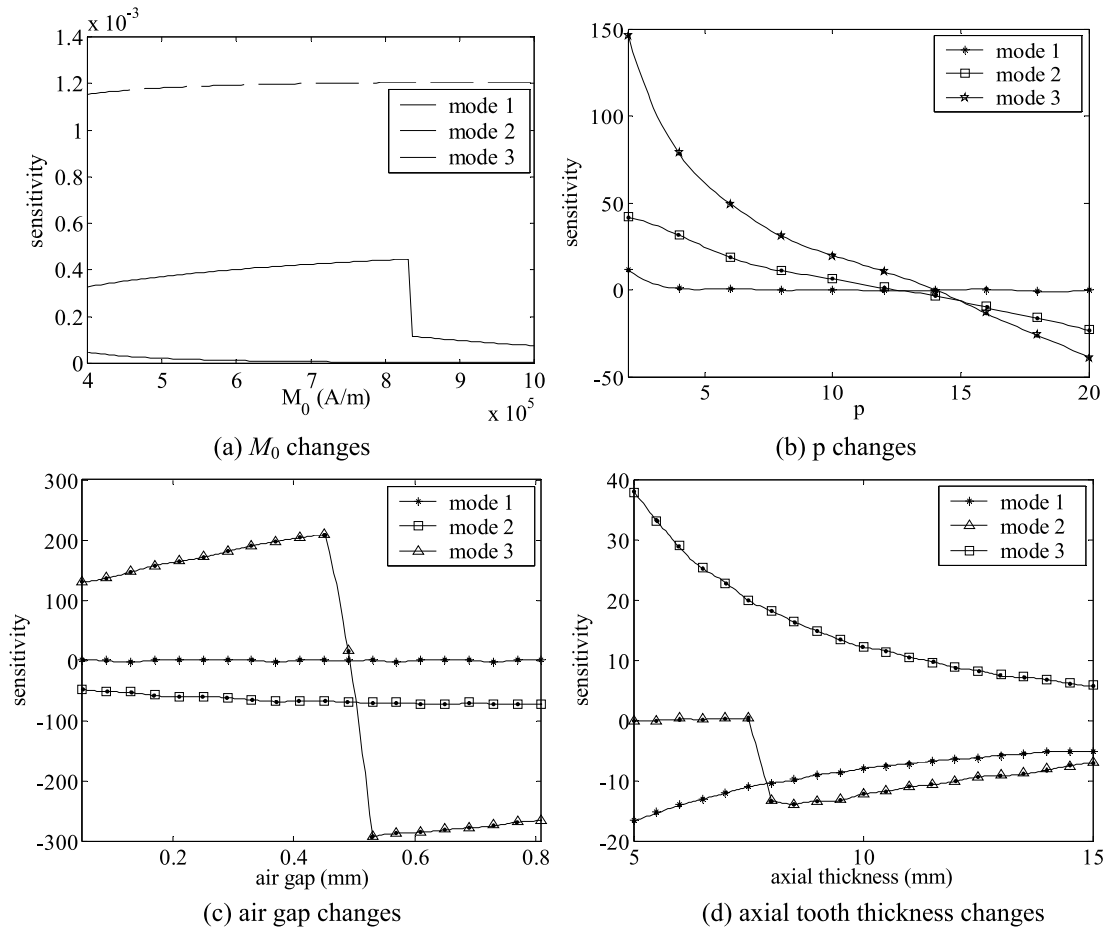
(a) M_0 changes (b) p changes

(c) air gap changes (d) axial tooth thickness changes

Fig. 12. Sensitivity to the system parameters for the planet modes.

(4) As the air gap grows, the 1st order natural frequency does not change nearly, the 2nd order natural frequency drops, and the 3rd natural frequency first grows, and then drops.

(5) As the tooth thickness grows, the 1st order natural frequency drops, the 2nd order natural frequency first does not change nearly, and then drops, and the 3rd natural frequency grows. However, the 3rd natural frequency grows more slowly with increasing the tooth thickness.

6. Conclusions

In this paper, a dynamic model for the magnetic planetary gear drive is proposed. Based on the model, the dynamic equations for the magnetic planetary gear drive are given. From the magnetic meshing forces and torques between the elements for the drive system, the tangent and radial magnetic meshing stiffness is obtained. Using these equations, the natural frequencies and vibration modes of the magnetic planetary gear drive are investigated. Results show:

(1) For the planetary gear number larger than two, the vibrations of the drive system include the torsion mode of the center elements, the translation mode of the center elements, and the planet modes.

(2) For the planetary gear number equal to two, the planet mode does not occur. Besides the torsion and translation modes of the center elements, two special modes occur. One is only for the translation of the crown gear which is called as the crown mode. Another is only for the translation of the sun gear which is called as the sun gear mode.
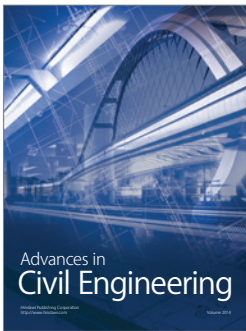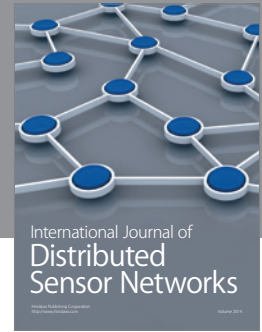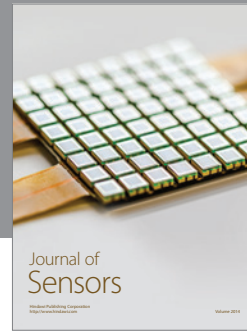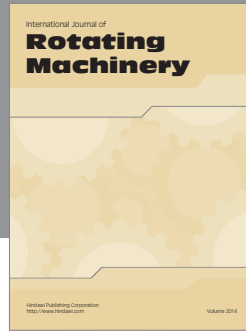
(3) The sensitivity parameter of the natural frequencies to the magnetization intensity of the magnetic tooth is small. It is large to the pole pair number of the worm coils or the air gap. It is moderate to the tooth thickness of the magnetic gear. This shows that the pole pair number and the air gap have more obvious effects on the natural frequencies than the magnetization intensity or the tooth thickness.

Acknowledgment

References

[1]   K. Tsurumoto and S. Kikuchi, New magnetic gear using permanent magnet, *IEEE Transactions on Magnetics* **23**(5) (1987), 3622–3624.

[2]   K. Tsurumoto, Generating mechanism of magnetic force in meshing area of magnetic gear using permanent magnet, *IEEE Translation Journal on Magnetics* **6**(6) (1991), 531–536.

[3]   M.H. Nagrial and J. Rizk, Design and performance of a magnetic gear, *IEEE International Magnetics Conference-2000 IEEE INTERMAG*, Toronto, Ont, 9–13 Apr 2000, pp. 644-648.

[4]   H. Zhao, Z. Yang and K. Huang, Torque characteristic analysis and optimal design of permanent-magnetic gears by using finite element method, *Proceedings of the International Conference on Mechanical Transmissions*, Chongqing, China, 5–9 Apr 2001, pp. 318–321.

[5]   H. Zhao, Z. Yang and J. Tian, Study on calculation method of the torque of permanent magnetic gears, *Chinese Journal of Mechanical Engineering* **37**(11) (2001), 69–70.

[6]   H. Zhao and Z. Yang, Three-dimensional analysis and calculation of the torque of permanent magnetic gears, *Transactions of the Chinese Society of Agricultural Machinery* **32**(6) (2001), 95–98.

[7]   F.T. Jorgensen, T.O. Andersen and P.O. Rasmussen, Two dimmensional model of a permanent magnet spur gear – A mathematical method used to model a parallel magnetised magnetic spur gear, *2005 IEEE Industry Applications Conference, 40th IAS Annual Meeting*, Hong Kong, China, 2–6 Oct 2005, pp. 261–265.

[8]   J. Tian, H. Deng and H. Zhao, Dynamic simulation study on the permanent thulium magnetism gear driving system, *China Mechanical Engineering* **17**(22) (2006), 2315–2318.

[9]   S. Kikuchi and K. Tsurumoto, Trial construction of a new magnetic skew gear using permanent magnet, *IEEE Transactions on Magnetics* **30**(6) (1994), 4767–4769.

[10]   S. Kikuchi and K. Tsurumoto, Design and characteristics of a new magnetic worm gear using permanent magnet, *IEEE Transactions on Magnetics* **29**(6) (1993), 2923–2925.

[11]   F.T. Joergensen, T.O. Andersen and P.O. Rasmussen, The cycloid permanent magnetic gear. Conference Record – IAS Annual Meeting (IEEE Industry Applications Society), *Conference Record of the 2006 IEEE Industry Applications Conference – Forty-First IAS Annual Meeting*, Tampa, FL, United States, 8–12 Oct 2006, pp. 373–378.

[12]   F.T. Jorgensen, T.O. Andersen and P.O. Rasmussen, The cycloid permanent magnetic gear, *IEEE Transactions on Industry Applications* **44**(6) (2008), 1659–1665.

[13]   K.H. Ha, Y.J. Oh and J.P. Hong, Design and characteristic analysis of non-contact magnet gear for conveyor by using permanent magnet, *37th IAS Annual Meeting and World Conference on Industrial applications of Electrical Energy*, Pittsburgh, PA, United States, 13–18 Oct 2002, pp. 1922–1927.

[14]   L.N. Jian, K.T. Chau and D. Zhang, A magnetic-geared outer-rotor permanent-magnet brushless machine for wind power generation, *Conference Record of the 2007 IEEE Industry Applications Conference 42nd Annual Meeting*, New Orleans, LA, United States, 23–27 Sep 2007, pp. 573–580.

[15]   L. Xu and X. Zhu, Magnetic planetary gear drive, *Proceedings of the Institution of Mechanical Engineers, Part C: Journal of Mechanical Engineering Science* **223**(9) (2009), 2167–2181.

[16]   C. Zhang, Machinery Hynamics(Second Edition). Peking:Higher Education Press, 2.

[17]   L. Jian and R.G. Parker, Analytical Characterization of the Unique Properties of Planetary Gear Free Vibration, *Journal of Vibration and Acoustics* **121**(3) (1999), 316–321.